Materials Research Bulletin 48 (2013) 1148–1154

Contents lists available at SciVerse ScienceDirect

Materials Research Bulletin

journal homepage: www.elsevier.com/locate/matresbu

Effect of $LiAlO_2$ nanoparticle filler concentration on the electrical properties of PEO–$LiClO_4$ composite

E.M. Masoud *, A.-A. El-Bellihi, W.A. Bayoumy, M.A. Mousa

Chemistry Department, Faculty of Science, Benha University, Benha, Egypt

ARTICLE INFO

Article history:
Received 9 May 2012
Received in revised form 4 December 2012
Accepted 5 December 2012
Available online 13 December 2012

Keywords:
A. Composites
D. Dielectric properties
D. Ionic conductivity

ABSTRACT

Nano-composite polymer electrolytes are receiving attention as potential candidates to be used as electrolyte membranes in lithium polymer batteries and other devices. In this work, polyethylene oxide–$LiClO_4$ based composite polymer electrolyte was prepared by solution casting method. The effect of $LiAlO_2$ nanoparticle ceramic filler concentration on the structure and electrical conduction of the composite was studied. Nano-$LiAlO_2$ was synthesized by sol–gel method. The samples were characterized using X-ray diffraction, Fourier Transmission-Infra Red, Differential Scanning Calorimetry, and tested by dielectric properties, Direct and Alternating current measurements as well as by impedance spectroscopy. All samples showed a behavior referring to an ionic conduction. Generally, the melting temperature of the polymer electrolyte decreased with filler concentration. Both thermal property and filler concentration influenced conductivity value. At room temperature, the highest ionic conductivity was 9.76×10^{-5} ohm^{-1} cm^{-1} for sample with a composition of $(LiAlO_2)_{1.5}$(polyethylene oxide)$_{11}$($LiClO_4$). All results were correlated and discussed.

1. Introduction

Solid polymer electrolyte (SPE) has attracted very much attention for applications in energy storage devices, such as batteries of different types and laptop computers [1]. The advantages of using SPE instead of liquid electrolytes are flexibility, no leakage and low self discharge in batteries. The most frequently used polymer is polyethylene oxide (PEO) because it can dissolve many inorganic salts and benefit structure for supporting ion migration [2]. However this polymer showed low ionic conductivity in the range of 10^{-7} ohm^{-1} cm^{-1} to 10^{-8} ohm^{-1} cm^{-1} which restricted the mobility of ions. Attempts have been made to increase the ionic conductivity of PEO by adding fillers, such as plasticizers or ceramic powders [3,4]. Addition of ceramic filler into polymer matrix results in reducing the glass transition temperature (T_g) and increasing the amorphous phases of the polymer matrix, therefore increases the ionic conductivity.

The ionic conduction of a polymer electrolyte is highly dependent on the crystallinity of the matrix and concentration of the added salt, but it is not clear if the conduction process involves all ions of the salt. The polymer–ceramic composite electrolytes are proposed to comprise of an assemblage of molecular dipoles whose orientations are dependent upon temperature and electric field. One of the major factors contributing to the conductivity is the orientation of these dipoles [5].

The study of dielectric relaxation behavior in ion conducting polymer composite materials has become an interesting area of active research for understanding the ionic transport properties of these materials. In order to gain a better understanding on ion dynamics and segmental relaxation, the conduction relaxation spectroscopy gives some valuable insights. Also how the relaxation dynamics are affected with salt concentration is very much important.

This paper was designed to analyze the effect of temperature and nano $LiAlO_2$ filler concentration on the electrical data of a $(PEO)_{12.5}(LiClO_4)$:$LiAlO_2$ to give more information to understand the origin of conduction enhancement in polymer ceramic composite electrolyte.

2. Experimental

Materials: Pure reagent materials of $LiNO_3$ (purity 99%, Merck), $Al(NO_3)_3$ (purity 99%, Merck), citric acid ($C_6H_8O_7$, purity 98%, Fluke), PEO (with an average molecular weight of 8×10^6, Sigma–Aldrich) and $LiClO_4$ (purity 99%, Sigma–Aldrich) were used as starting materials to prepare nano filler and polymer nano composite electrolyte.

* Corresponding author. Tel.: +20 1203532343.
E-mail address: emad_masoud1981@yahoo.com (E.M. Masoud).

0025-5408/$ – see front matter © 2012 Elsevier Ltd. All rights reserved.
http://dx.doi.org/10.1016/j.materresbull.2012.12.012

2.1. Preparation of nano $LiAlO_2$ filler

Lithium aluminate nano particles filler was prepared by citrate-based sol–gel method [6]. 0.5 mol lithium nitrate and 0.5 mol aluminum nitrate were firstly dissolved in 300 ml distilled water, then 1 mol citric acid was added to the above solution .The molar amount of citric acid was equal to total molar amount of metal nitrates in the solution. Ammonium hydroxide was slowly added to adjust the pH value of the solution in the range of 8–9 and also to stabilize the nitrate–citrate solution. During this procedure, the solution was kept at room temperature and continuously stirred. The obtained transparent sol was kept at 80 °C to get a gel, which was then dried at 110 °C for 10 h. Finally, the precursor powder was calcinated at 950 °C for 6 h.

2.2. Preparation of polymer nano composite electrolytes

The composite samples were synthesized by the conventional solution cast technique. PEO and $LiClO_4$ were dissolved in acetonitrile and magnetically stirred to get a homogeneous solution. An appropriate weight of nano lithium aluminate was then added to the solution and stirred for 6 h to get a white viscous solution with high homogeneity. After that, the viscous solution was poured into a peter dish and left to dry at room temperature for two days to allow the solvent to be slowly evaporated. All the films obtained with different concentrations of filler were then dried under a vacuum for 10 h and kept in a desiccator.

2.3. Characterization of samples

X-ray diffraction was performed on the investigated samples using a Philips X-ray diffractometer (Model PW 1710) with CuKα radiation (λ = 1.54 Å) in the range of $2\theta = 4–60^\circ$. Thermal analysis was performed on the investigated samples in air atmosphere and at a temperature range of 298–353 K using differential scanning calorimetric technique (DSC) by Shimadzu DSC-60H. FT-IR spectra of the samples were recorded in the range of 400–4000 cm^{-1} using KBr pellet technique on IR-Brucker, Vector 22, Germany. The electrical measurements were carried out on the samples in the form of films. The two parallel surfaces of the films were coated with silver paste to ensure good electrical contact. Each investigated sample was located in a sample holder inside a cryostat with a temperature controller of ±0.01 °C accuracy. The dielectric properties, DC-, AC-electrical conductivity as well as impedance spectra were measured at a constant voltage (1 volt) by using programmable automatic LCR bridge (Model RM 6306 Phillips bridge).

3. Results and discussion

Fig. 1 shows X-ray diffraction patterns of $LiAlO_2$, PEO, $(LiAlO_2)_x(PEO)_{12.5-x}(LiClO_4)$ (x = 0, 0.5, 1, 1.5, and 2 mol). The spectra of $LiAlO_2$ is a typical XRD pattern for $LiAlO_2$ with a tetragonal structure as indexed in the standard data (JCPDS card No. 74-2232, a = 2.800 Å and c = 14.21 Å) [7]. XRD line broadening was used to estimate the grain size of the powders according to Scherrer formula [8]:

$$D = \frac{0.9\lambda}{\beta \cos\theta} \quad (1)$$

where D is the average diameter of the grains, λ is the wavelength of X-ray, θ is the Bragg angle and β is the full width half maximum in radians. The results showed an average crystalline size of about 41 nm. It can be also seen by Fig. 1 that the characteristic diffraction peaks of crystalline PEO (2θ = 19 and 23.5°) become

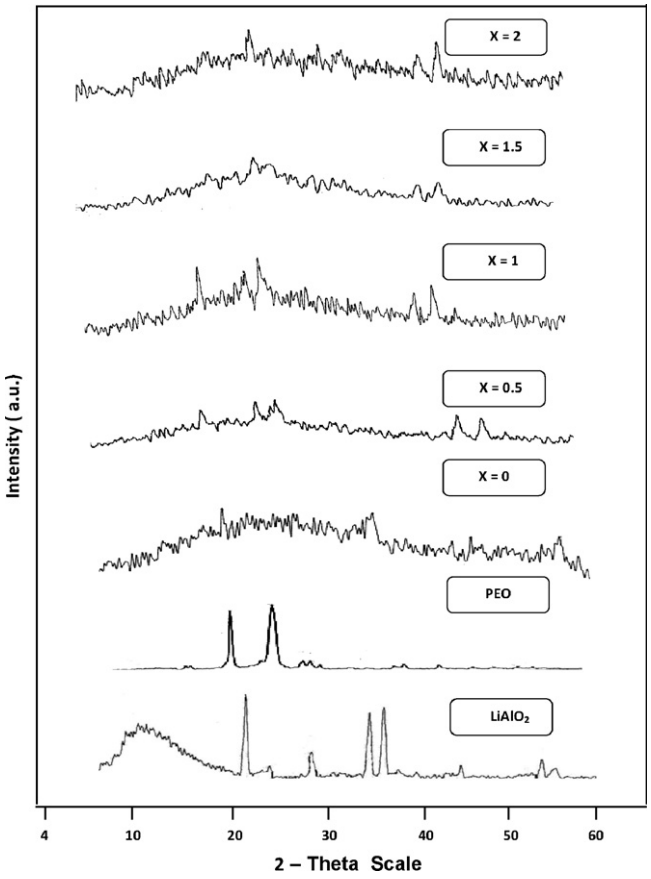

Fig. 1. XRD patterns of $LiAlO_2$, pure PEO and $(LiAlO_2)_x(PEO)_{12.5-x}(LiClO_4)$ (x = 0, 0.5, 1, 1.5, 2 mol).

weaker and broader with the addition of $LiClO_4$ and inorganic filler $LiAlO_2$. The peaks corresponding to nano $LiAlO_2$ in the composite have not been observed because their peak intensities became very low and broad as shown in Fig. 1. The decrease in the crystallinity of PEO is resulting from the coordination interactions between the ether O atoms of PEO and Li^+ [9]. This means that the mediators may exist in a highly divided or amorphous state or present in a completely dispersed state in the PEO/$LiClO_4$ electrolyte. This result may also indicate that the structure of the PEO polymer electrolyte has locally changed into a disordered form as evidenced from crystallinity percent values (X_c) calculated from DSC (Fig. 2). In other words, the amorphous phase volume fraction of the PEO polymer electrolyte increased with amount of $LiAlO_2$ into the polymer matrix.

DSC technique was used to further study the effect of fillers on the crystallization behavior of PEO. DSC plots of pure PEO and $(LiAlO_2)_x(PEO)_{12.5-x}(LiClO_4)$ (x = 0, 0.5, 1, 1.5, and 2 mol) composites are displayed in Fig. 2. For all samples, the endothermic peak between 50 and 70 °C is corresponding to melting of the crystalline PEO. Crystallinity (X_c) was calculated as a ratio of enthalpy of melting of the composite (ΔH_c) to enthalpy of melting of the pure crystalline PEO phase (ΔH_p = 203 J/g) [10] by the following equation:

$$X_c = \frac{H_c}{H_p} \quad (2)$$

The calculated X_c-values and the data obtained from DSC thermograms are summarized in Table 1. From which it can be seen that each of the melting temperature (T_m) and crystallinity of PEO (X_c) obviously decrease with $LiClO_4$ and inorganic filler

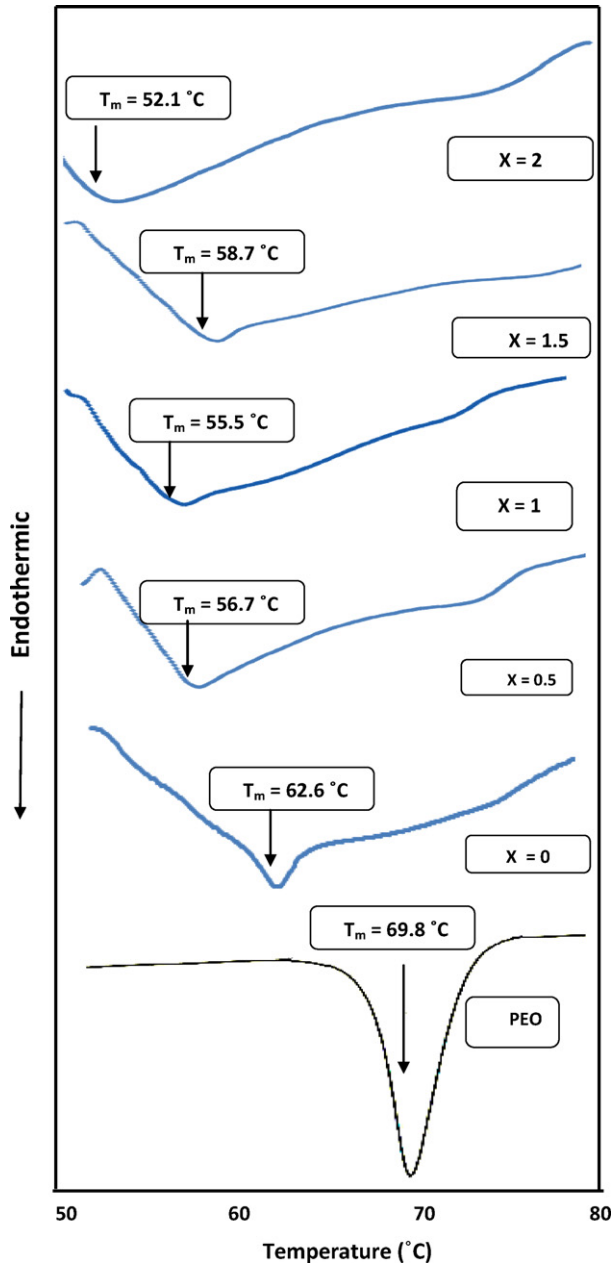

Fig. 2. DSC curves of pure PEO and $(LiAlO_2)_x(PEO)_{12.5-x}(LiClO_4)$ (x = 0, 0.5, 1, 1.5, 2 mol).

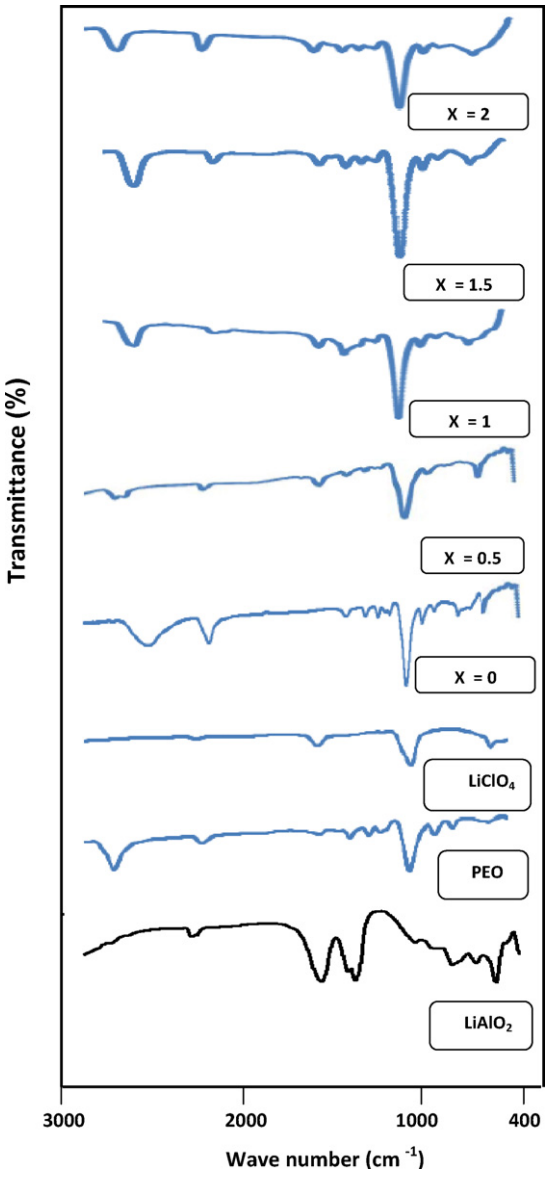

Fig. 3. IR patterns of $LiAlO_2$, PEO, $LiClO_4$ and $(LiAlO_2)_x(PEO)_{12.5-x}(LiClO_4)$ (x = 0, 0.5, 1, 1.5, 2 mol).

($LiAlO_2$) addition. This refers to an increase in the enhanced segmental motion and flexibility of PEO host polymer with increasing the amount of $LiAlO_2$ filler. It means that the inert filler incorporation in our samples acts as a solid plasticizer capable of enhancing the transport properties.

Table 1
Melting temperatures (T_m), melting enthalpy (ΔH_m) and crystallinity (X_c) for $(LiAlO_2)_x(PEO)_{12.5-x}$ ($LiClO_4$).

X (mol)	T_m (°C)	H_m (J/g)	X_c (%)
Pure PEO	69.8	139.1	68.5
0	62.6	52.3	25.8
0.5	56.7	28.6	14.1
1	55.5	138.8	68.4
1.5	58.7	97.7	48.1
2	52.1	110.7	54.5

IR spectra of investigated samples are shown in Fig. 3. Comparing the spectra of pure PEO with its composites showed that some bands of PEO are affected due to the incorporation of $LiClO_4$ and nano $LiAlO_2$ into PEO polymeric matrix. The metal oxygen band stretching frequency in pure $LiAlO_2$, at 538 cm^{-1}, was shifted to 587 cm^{-1} in the composite species. This may be attributed to Van der-Waals interaction between $LiAlO_2$ and PEO polymeric molecule. For C–O–C vibration modes, at 1050–1160 cm^{-1} and 800–1000 cm^{-1}, significant changes were observed in each of the width and intensity of the vibration band due to $LiClO_4$ salt and nano $LiAlO_2$ filler addition. This is attributed to the electrostatic interactions occurring between Li^+ metal ion with the ether oxygen found in PEO macromolecules [11,12]. This interaction may weaken the bond strengths of C–O–C in PEO macromolecule.

3.1. DC-electrical conductivity

The temperature dependence of DC-electrical conductivity for the investigated samples is studied at a temperature range of

Table 2
DC and bulk conductivity (σ_{dc}, σ_b) data for $(LiAlO_2)_x(PEO)_{12.5-x}$ ($LiClO_4$) at room temperature (293 K).

X (mol)	E_a (eV)	σ_{dc} ($ohm^{-1}\,cm^{-1}$)	σ_b ($ohm^{-1}\,cm^{-1}$)	E_a (eV)
Pure PEO	0.40	1.25×10^{-9}	7.00×10^{-7}	0.33
0	0.46	1.55×10^{-7}	1.60×10^{-4}	0.55
0.5	0.18	4.83×10^{-5}	2.82×10^{-4}	0.57
1	0.61	3.00×10^{-5}	7.84×10^{-5}	1.07
1.5	0.16	9.76×10^{-5}	6.5×10^{-4}	0.45
2	0.09	3.41×10^{-5}	9.39×10^{-5}	1.05

298–318 K (Fig. 4). The overall feature of the plots is almost similar for all investigated composites. The conductivity data are summarized and given in Table 2. The conductivity increase with temperature (Fig. 4) can be attributed to viscosity decreasing and hence increasing the flexibility chain of the sample [13]. Inspection of Table 2 shows that the $LiAlO_2$ filler free sample has an activation energy (0.46 eV) higher than that for the $LiAlO_2$ filler samples (0.09–0.18 eV). The decrease of activation energy can be attributed to an increase in the amorphous nature of the composite sample that will facilitate Li^+ ion motion in the polymer network [14], as shown later in the impedance results.

Table 2 also shows that addition of nano $LiAlO_2$ in the PEO–$LiClO_4$ matrix causes a high enhancement in the conductivity of the composite electrolyte. The electrical conductivity attained a value 100 times higher than that of the based polymer electrolyte. Increase in conductivity may be attributed to an increased flexibility of the composite by introducing $LiAlO_2$ into PEO matrix, due to the high interface area between the matrix and the dispersed nano $LiAlO_2$ particles [15–17]. Moreover, increasing the amorphous state within the PEO-matrix, due to nano $LiAlO_2$ addition (as evidenced by XRD section), causes an enhancement in the segmental motion of the polymer chains and hence increases the conductivity.

The small particle size of $LiAlO_2$ in our samples is more efficient for conductivity enhancement than that found for a similar system containing filler particle size of 1–4 μm [18]. This indicates that the particle size in nano-range plays an important role in enhancing the polymer electrolyte conductivity.

Fig. 5 shows a non linear increase in conductivity of the composite with increasing the concentration of nano $LiAlO_2$ filler. The two maxima appearing in Fig. 5 have been also reported by few workers for other composite systems of ion conducting gel polymer electrolyte [19] and also for solvent free composite polymer electrolytes [20–22]. The first conductivity maximum is possibly due to the dissociation of ion aggregates salt into the free ions with $LiAlO_2$ nano-particles addition, whereas the second conductivity maximum is related to the composite effect and explained on the basis of formation of a conducting interfacial space–charge double layer between the nano sized $LiAlO_2$ particles and polymer electrolytes [23,24]. The decrease in conductivity at $x = 1$ mol can be discussed in view of molecular motion of PEO chain where it can strongly affect the movement of ions where Lewis acid–base interactions between the polar surface groups of $LiAlO_2$ and the electrolyte ions at high content of filler lead to the gauche arrangement of PEO backbone. The gauche conformation can decrease the segmental motion of PEO and as a result the conductivity decreases. Above 1 mol, the high conducting regions

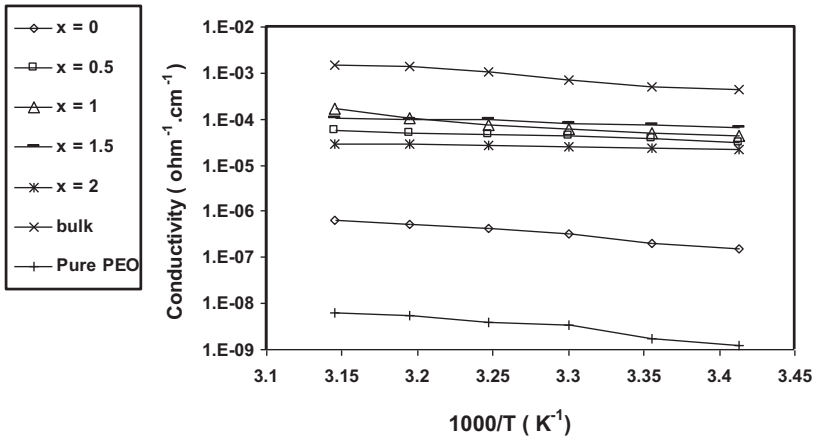

Fig. 4. Temperature dependence of both DC-conductivity for composite samples with different x values and bulk conductivity at $x = 1.5$ mol.

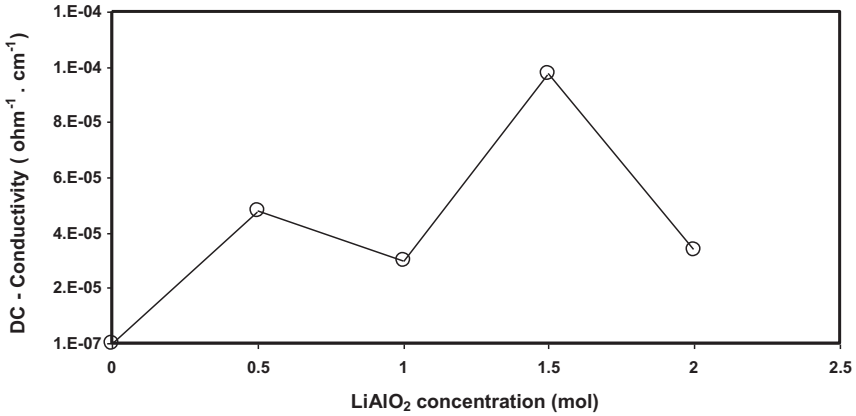

Fig. 5. $LiAlO_2$ concentration dependence of dc-conductivity (σ_{dc}) for $(LiAlO_2)_x(PEO)_{12.5-x}(LiClO_4)$ ($x = 0$, 0.5, 1, 1.5, 2 mol) at room temperature (293 K).

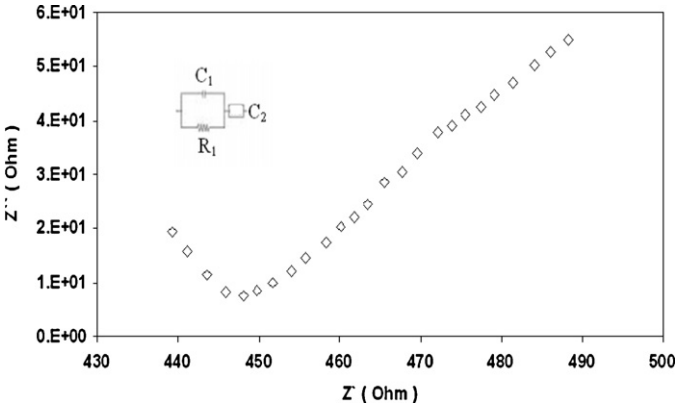

Fig. 6. Plot of Z'' versus Z' for $(LiAlO_2)_{1.5}(PEO)_{11}(LiClO_4)$ at room temperature (293 K).

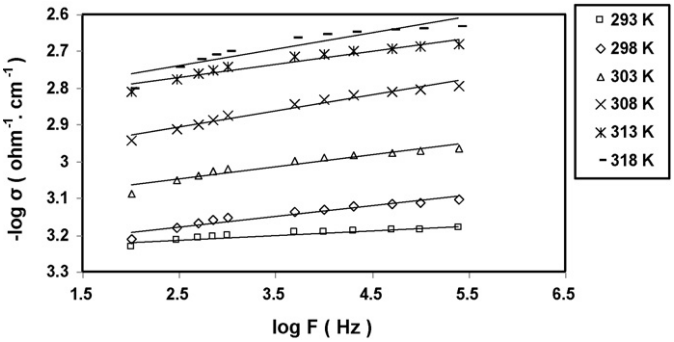

Fig. 7. Variation of AC-electrical conductivity with frequency at different temperatures for $(LiAlO_2)_{1.5}(PEO)_{11}$ $(LiClO_4)$.

are interconnected to enhance the conductivity up to 1.5 mol. The conductivity decrease after the maximum second conductivity (Fig. 5) is generally related to the blocking effect of filler particles, which hinders the motion of mobile ions [25].

The conductivity results (Table 2) showed a highest conductivity value for the sample containing 1.5 mol nano $LiAlO_2$ as it contains the highest amorphous state (see XRD) which facilitates the transport of ionic charge carriers, as will be seen later. Also, the other samples showed DC-conductivity order [$(\sigma_{DC}\ (x = 0.5) < \sigma_{DC}\ (x = 2) < \sigma_{DC}\ (x = 1)$], which goes in a logic reverse one of crystallinity values [$X_c\ (x = 0.5) < X_c\ (x = 2) < X_c\ (x = 1)$].

It is well known that, the electrical devices that work over a wide temperature range should have uniform conductivity with low activation energy [26]. Therefore, according to this view and the results obtained, the composite system containing 1.5 mol nano $LiAlO_2$ was chosen for further study using AC-conductivity,

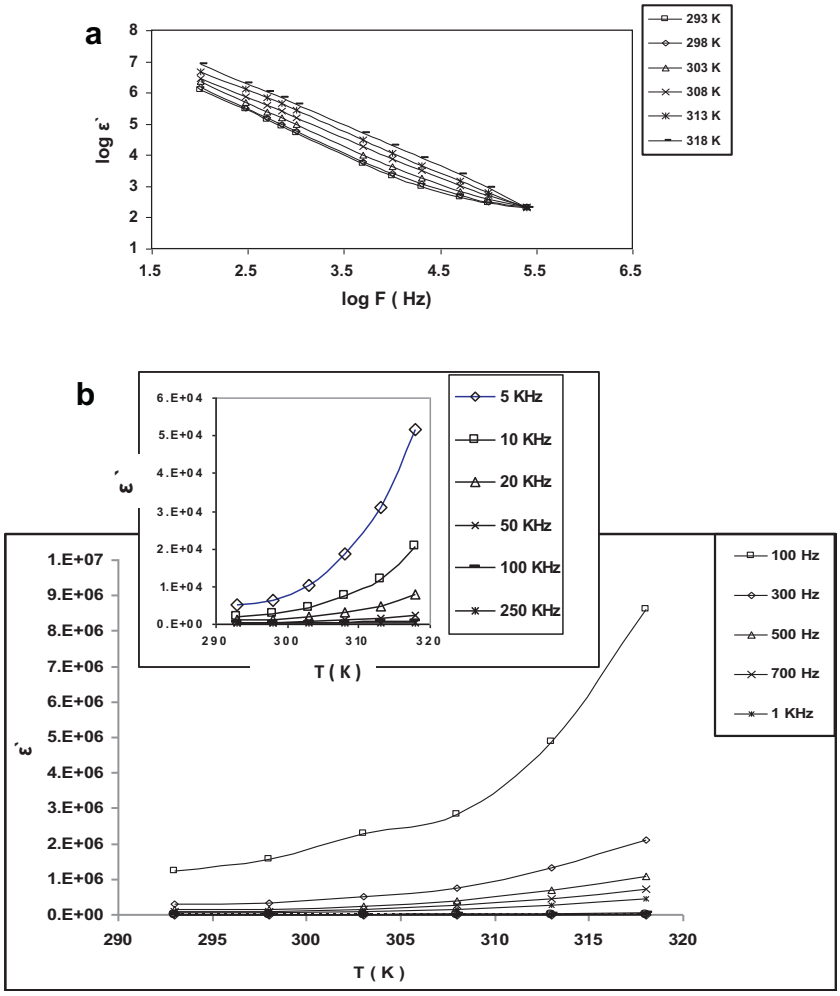

Fig. 8. (a) Variation of dielectric constant with frequency at different temperatures for $(LiAlO_2)_{1.5}(PEO)_{11}(LiClO_4)$. (b) Variation of dielectric constant with temperature at different frequencies for $(LiAlO_2)_{1.5}(PEO)_{11}$ $(LiClO_4)$.

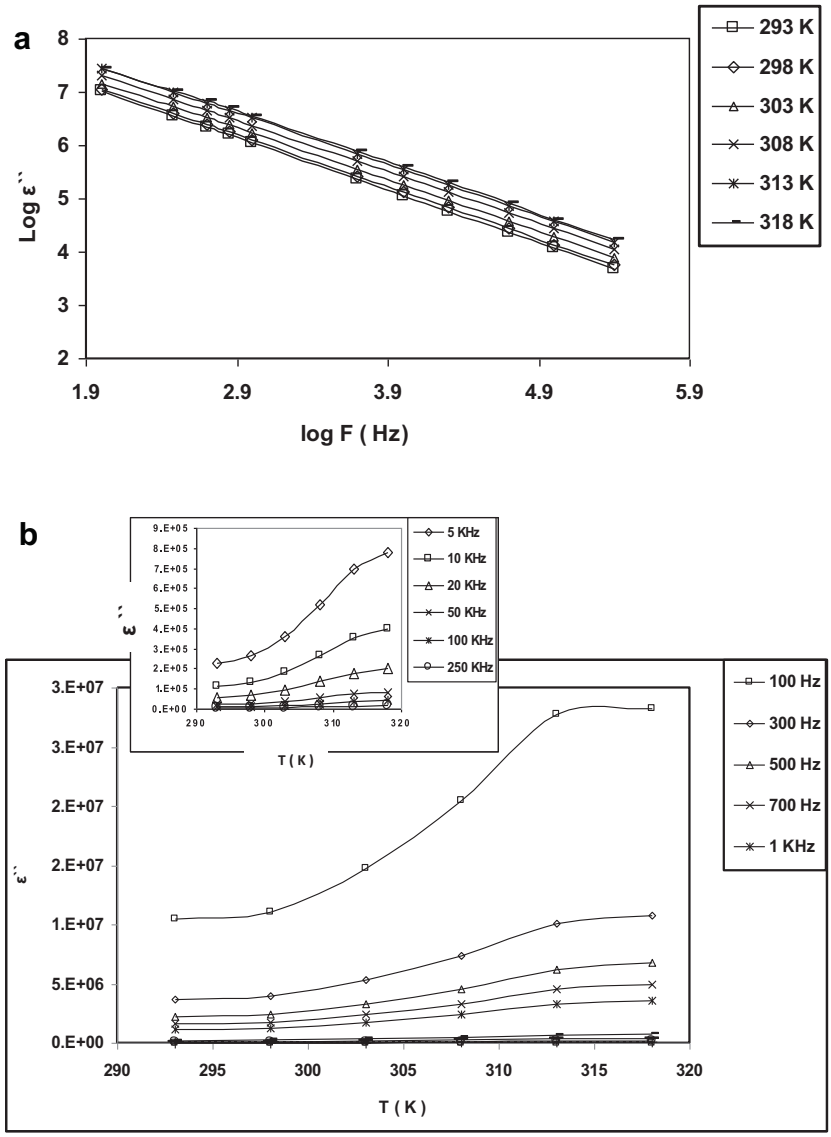

Fig. 9. (a) Variation of dielectric loss with frequency at different temperatures for $(LiAlO_2)_{1.5}(PEO)_{11}(LiClO_4)$. (b) Variation of dielectric loss with temperature at different frequencies for $(LiAlO_2)_{1.5}(PEO)_{11}$ $(LiClO_4)$.

dielectric behavior, and impedance character. This will give us more information on the dipoles of the studied samples.

3.2. Impedance spectroscopy analysis

Impedance plots (Z' Vs. Z'') in the complex plane for $(LiAlO_2)_{1.5}(PEO)_{11}(LiClO_4)$ at different temperatures showed a similar behavior. A typical plot is shown in Fig. 6, which demonstrates a depressed semicircular portion followed by a spike. This spike refers to an ionic conductivity and it is characteristic of a blocking double layer capacitance whose magnitude can be estimated from any position on the spike using the equation. $Z'' = 1/2\pi f C_{di}$, where f is the applied frequency and C_{di} is the capacitance at the frequency f. The ionic conductivity of the solid polymer nano composite electrolyte $(LiAlO_2)_{1.5}(PEO)_{11}(LiClO_4)$ was derived by the ac impedance analysis. The high depression of the semicircular portion at high frequencies, in complex impedance, is a result of the ionic conductivity increase with frequency increasing [15]. The equivalent circuit of the polymer nano composite electrolyte system is determined by the complex impedance spectrum and given in Fig. 6, where R_1 is the bulk resistance of the electrolyte, C_1 is the bulk capacity of the electrolyte and C_2 is a capacity of bulk electrode–electrolyte interface. The bulk ionic conductivity of 6.5×10^{-4} ohm^{-1} cm^{-1} at room temperature was calculated using the equation $\sigma_b = L/R_bA$, where L is the thickness of the polymer nano composite electrolyte film and A is its surface area. The resistance of the electrolyte (R_b) was determined from the intercept of the impedance spectrum on the Z' real axis. The temperature dependence of the bulk conductivity showed Arrhenius behavior (Fig. 4) as that reported by dc-conductivity. The bulk conductivity data are also reported in Table 2. The difference between dc and impedance data is attributed to the grain boundaries present between the particles.

3.3. AC-conductivity

In order to give information on the type of polarization present in $(LiAlO_2)_{1.5}(PEO)_{11}(LiClO_4)$ sample, the ac-electrical conductivity (σ_{ac}), at temperatures between 293 and 318 K and a frequency range of 10^2–10^5 Hz was studied. The results are illustrated in Fig. 7. It can be seen that the conductivity increases with each of the frequency and temperature. The increase in σ_{ac} with temperature can be explained on the basis that raising the temperature causes more structure relaxation and releasing more

of Li^+ ions attached to oxygen of PEO to become more mobilized. This may be also due to increasing the drift mobility and hopping frequency of charge carriers. The frequency dependence of conductivity is also attributed to the change occurring in the mobility of charge carriers.

3.4. Dielectric permittivity and loss studies

The frequency dependence of dielectric constant (ε') at different temperatures for $(LiAlO_2)_{1.5}(PEO)_{11}(LiClO_4)$ sample is shown in Fig. 8a. It can be seen that ε' decreases as frequency increases. This decrease is relatively sharp at lower frequencies and slow at higher ones. The decrease of dielectric permittivity with frequency increasing can be associated to the inability of dipoles to rotate rapidly leading to a lag between frequency of the oscillating dipole and that of the applied field [27]. The dielectric permittivity obtained in our system ($\varepsilon' = 1.22 \times 10^6$, at room temperature) is higher than that of the other compositions of our polymer electrolytes samples (ε' lies in the range of 9.8×10^3–2.93×10^5, at room temperature). Such high dielectric constant values in that sample can be attributed to the high ionic conductivity on account of the presence of $LiAlO_2$ nano particles and its good distribution within the matrix of polyethylene oxide and also due to the good interactions between the Lewis acidic sites on the surface of those particles and lithium perchlorate ions [28]. When the temperature rises, dielectric constant also enhances due to the facilitation in orientation of dipoles within the matrix of PEO [29].

The temperature dependence of dielectric constant at different frequencies is shown in Fig. 8b. The variation of dielectric constant with temperature can be divided into two ranges. In the lower temperatures range (from 293 to 303 K), the change in dielectric constant is weakly dependent on temperature but in the higher ones (from 303 to 318 K), the dielectric constant is strongly dependent on temperature. The increase of dielectric constant with temperature is generally attributed to two mechanisms. The first is to the decrease of viscosity of the polymer nano composite electrolyte [29] and the second is to the dissolving of any small concentration of crystalline and semi-crystalline phases into the amorphous phase [27]. This is in turn influences the polymer dynamics and thus the dielectric behavior. The presence of the two ranges in Fig. 8b may be attributed to the effect of the two mechanisms. Whereas, at lower temperature range, the viscosity is high and crystalline phases are present, thus, the dielectric behavior is weakly dependent on temperature. While at higher temperatures, the opposite trend is predominate.

Fig. 9a and b shows the variation of dielectric loss (ε'') with frequency and temperature for $(LiAlO_2)_{1.5}(PEO)_{11}(LiClO_4)$ sample. The observed behaviors are similar to that found for dielectric constant. Where the dielectric loss decreased with increasing the frequency due to high periodic reversal of the field at the interface; the contribution of charge carriers (ions) towards the dielectric loss decreases with frequency increasing and this can be due to the reduction of the diffusion of the ions in the polymer matrix with increasing the frequency. The increase of dielectric loss with temperature increasing can be also attributed to the relaxation of the dipoles in co-operation with the resulting drop in the relaxation time.

4. Conclusions

Nano $LiAlO_2$ filler with an average particle size of 41 nm was prepared by sol–gel method. Polymer electrolyte based on $(PEO)_{11.5}(LiClO_4)$ with nano $LiAlO_2$ filler has been developed and examined using XRD, FT-IR, DSC, dielectric properties, DC-, AC-conductivity and impedance analysis. Shifts, broadening and reduction in intensity of FT-IR-bands confirm dissolution of the metal salt in the polymer matrix. The DSC analysis revealed to a change in the crystallinity and melting points of the composite samples with different filler concentrations. The incorporation of the inert filler reduces the crystallinity of the host polymer and acts as a solid plasticizer capable of enhancing the transport properties. All composite samples showed an ionic conductivity, in which $LiAlO_2$ nano-particles addition enhances the conductivity of the based polymer, at room temperature, by 100 times. The $LiAlO_2$ content dependence of ionic conductivity reveals further changes in the amorphous state and viscosity; these two major factors influence the ion mobilities. Sample containing 1.5 mol nano $LiAlO_2$ showed a conductivity of $9.76 \times 10^{-5}\ ohm^{-1}\ cm^{-1}$ at room temperature, which is the highest conductivity value for all investigated samples. The electrical properties of this sample showed dielectric permittivity and loss values of 1.22×10^6 and 1.05×10^7, respectively, at room temperature. These high values of DC-conductivity, dielectric permittivity and dielectric loss at room temperature lead to make the sample as a promising material for lithium battery as an application in the solid state electrochemical devices.

References

[1] A. Karmakar, A. Ghosh, Curr. Appl. Phys. 12 (2012) 539.
[2] A. Ghosh, P. Kofinas, Electrochemical Society Transactions 11 (2008) 131.
[3] A.G. Bishop, D.R. Macfarlane, D.M.C. Naughton, M. Forsyth, J. Phys. Chem. 100 (1996) 2237.
[4] E. Quartarone, P. Mustarelli, A. Magistris, Solid State Ionics 110 (1998) 1.
[5] B. Kumar, L.G. Scanlon, R.J. Spry, J. Power Sources 96 (2) (2001) 337.
[6] R.B. Khomane, A. Agrawal, B.D. Kulkarni, Mater. Lett. 61 (2007) 4540.
[7] L. Hu, Z. Tang, Z. Zhang, J. Power Sources 166 (2007) 226.
[8] H.P. Klug, L.E. Alexander, X-ray Diffraction Procedures, Wiley, New York, 1970.
[9] J. Xi, X. Qiu, X. Ma, Solid State Ionics 176 (2005) 1249.
[10] B. Wiunderlieh, Macromolecular Physics, vol. 3, Academic Press, New York, 1980, p. 67.
[11] B.L. Papke, M.A. Ratner, D.F. Shriver, J. Electrochem. Soc. 129 (1982) 1434.
[12] S.J. Wen, T.J. Richrdson, D.I. Ghantous, K.A. Striebel, P.N. Ross, E.J. Cairns, J. Electroanal. Chem. 408 (1996) 113.
[13] K. Tsunemi, H. Ohno, E. Tsuchida, Electrochim. Acta 28 (6) (1983) 833.
[14] R. Baskaran, S. Selvasekarapandian, N. Kuwata, J. Kawamura, T. Hattori, J. Phys. Chem. Sol. 68 (2007) 407.
[15] L. Fan, Z. Dang, G. Wei, C. Nan, M. Li, Mater. Sci. Eng. B 99 (2003) 340.
[16] J. Maier, Solid State Ionics 75 (1995) 139.
[17] W. Wieczorek, D. Raducha, A. Zalewska, J. Phys. Chem. B 102 (1998) 8725.
[18] F. Croce, B. Scrosati, G. Mariotto, Chem. Mater. 4 (1992) 134.
[19] J.P. Sharma, S.S. Sekhon, Solid State Ionics 178 (2007) 439.
[20] B.K. Choi, K. Shin, Solid State Ionics 86–88 (1996) 303.
[21] S.A. Hashmi, H.M. Upadhayaya, A.K. Thakur, in: B.V.R. Chodari, W. Wang (Eds.), Solid State Ionics: Materials and Devices, vol. 461, World Scientific, Singapore, 2000.
[22] G.P. Pandey, S.A. Hashmi, R.C. Agrawal, Solid State Ionics 179 (2008) 543.
[23] J. Maier, Solid State Ionics 70–71 (1994) 43, Prog. Solid State Chem. 23 (1995) 171.
[24] B. Kumar, J. Power Sources 135 (2004) 215.
[25] B. Kumar, S. Nellutla, J.S. Thokchom, C. Chen, J. Power Sources 160 (2006) 1329.
[26] J.M.G. Cowie, G.H. Spence, Solid State Ionics 109 (1998) 139.
[27] A. Awadhia, S.K. Patel, S.L. Agrawal, Prog. Cryst. Growth Character. Mater. 52 (2006) 61.
[28] H.M. Xiong, X. Zhao, J.S. Chen, J. Phys. Chem. B 105 (2001) 10169.
[29] C.A. Finch, Polyvinyl Alcohol: Properties and Applications, John Wiley & Sons Ltd., London, 1973.